NIH Public Access
Author Manuscript

Phospholipid scramblase 1 mediates type I interferon-induced protection against staphylococcal α-toxin

Miroslaw Lizak[1] and **Timur O. Yarovinsky**[1,*]

[1] Section of Cardiovascular Medicine, Department of Internal Medicine, Yale University School of Medicine, New Haven, CT, USA.

Summary

The opportunistic gram-positive pathogen *Staphylococcus aureus* is a leading cause of pneumonia and sepsis. Staphylococcal α-toxin, a prototypical pore-forming toxin, is a major virulence factor of *S. aureus* clinical isolates and lung epithelial cells are highly sensitive to α-toxin's cytolytic activity. Type I interferon (IFN) signaling activated in response to *S. aureus* increases pulmonary cell resistance to α-toxin but the underlying mechanisms are uncharacterized. We show that IFNα protects human lung epithelial cells from α-toxin-induced intracellular ATP depletion and cell death by reducing extracellular ATP leakage. This effect depends on protein palmitoylation and induction of phospholipid scramblase 1 (PLSCR1). IFNα-induced PLSCR1 associates with the cytoskeleton after exposure to α-toxin and cellular depletion of PLSCR1 negates IFN-induced protection from α-toxin. PLSCR1-deficient mice display enhanced sensitivity to inhaled α-toxin and an α-toxin-producing *S. aureus* strain. These results uncover PLSCR1 activity as part of an innate protective mechanism to a bacterial pore-forming toxin.

Introduction

Staphylococcus aureus is an opportunistic gram-positive pathogen and the leading cause of severe and life-threatening infections, including pneumonia and sepsis (Kallen et al., 2010; Schreiber et al., 2011). Many clinical isolates of *S. aureus* produce α-toxin, a prototypical pore-forming toxin and a major virulence factor (Bartlett et al., 2008; Menzies and Kernodle, 1996; O'Reilly et al., 1986; Wilke and Bubeck Wardenburg, 2010). Human epithelial cells express ADAM10, a high-affinity protein receptor for α-toxin, which makes them intrinsically sensitive to the cytotoxic effects of α-toxin (Wilke and Bubeck Wardenburg, 2010). Formation of α-toxin pores in the plasma membrane of sensitive cells leads to major changes in the gradients of ions across the membrane, depletion of intracellular ATP, activation of pro-inflammatory cascades, and ultimate cell death (Bhakdi and Tranum-Jensen, 1991; Craven et al., 2009; Prevost et al., 2001; Ratner et al., 2006; Rose et al., 2002). Excessive inflammation and death of respiratory epithelial cells triggered by α-toxin during pneumonia contribute to acute lung injury and worsen the outcome of infection (Bartlett et al., 2008; Bubeck Wardenburg and Schneewind, 2008; Rose et al., 2002). Neutralization of the cytolytic activity of α-toxin protects animals from *S. aureus* (Bubeck Wardenburg and Schneewind, 2008; Kennedy et al., 2010; McCormick et al., 2009; Menzies

[*] Address correspondence to: Dr. Timur Yarovinsky, Yale University School of Medicine, Department of Internal Medicine, Section of Cardiovascular Medicine, 300 George Street, Ste. 750, New Haven, CT 06511; timur.yarovinsky@yale.edu..

and Kernodle, 1996; Ragle and Bubeck Wardenburg, 2009), suggesting that α-toxin is a promising target for intervention during staphylococcal infections.

Cellular defense against α-toxin and other pore-forming toxins relies on constriction of the α-toxin pores (Valeva et al., 2000), activation of mitogen-activated protein kinases (Husmann et al., 2006), induction of lipogenic genes via activation of sterol response element binding proteins (SREBP) by caspase-1 (Gurcel et al., 2006), and accelerated endocytosis and exocytosis (Husmann et al., 2009; Idone et al., 2008). Further characterization of host-intrinsic mechanisms of resistance to α-toxin should facilitate development of new therapeutic approaches for staphylococcal infection.

We have previously reported that type I interferons (IFNs) increase cell resistance to α-toxin, presumably via induction of interferon-regulated genes involved in lipid metabolism (Yarovinsky et al., 2008). However, activation of type I IFN signaling by staphylococcal protein A increased inflammation in the lungs (Martin et al., 2009). These opposing effects of I IFNs may be exerted through transcriptional regulation of distinct subsets of IFN-regulated genes. Therefore, it is important to identify which IFN-regulated genes and pathways are necessary for protection from α-toxin.

In this study, we focused on human lung epithelial cells since they are highly sensitive to α-toxin and represent the first line of defense against *S. aureus* during respiratory infections. We demonstrated that IFNα protects human lung epithelial cells from α-toxin-induced cell death by reducing release of cellular ATP into extracellular space. Using an ATP-based cell viability screening assay and bioinformatics analyses, we found that IFNα-induced protection from α-toxin is dependent on protein palmitoylation and induction of phospholipid scramblase 1 (PLSCR1). Increased expression of PLSCR1 has been previously implicated in bidirectional translocation of membrane phospholipids across plasma membrane and amplification of transcriptional responses to type I IFNs (Dong et al., 2004; Stout et al., 1997; Zhou et al., 2000). Here we show that IFNα-induced protection from α-toxin correlates with accumulation of PLSCR1 in the cytoskeleton-associated protein fractions.

Results

IFNα reduces α-toxin-induced cell death and release of extracellular ATP

Exposure of human primary small airway epithelial cells (SAEC) to staphylococcal α-toxin for 24 h resulted in significant cell death, which was preceded by rapid depletion of intracellular ATP (Figure 1). Pretreatment of SAEC with IFNα for 24 h significantly inhibited depletion of ATP and reduced cell death triggered by α-toxin. Although higher concentrations of α-toxin (0.5-2.5 µg/ml) were required to trigger ATP depletion in A549 cells, it was similarly inhibited by IFNα pretreatment (Figure 1D). Pretreatment with IFNα also inhibited ATP depletion from A549 cells incubated with conditioned medium from α-toxin-producing strain of *S. aureus* (Figure 1E-F). These data indicate that type I IFNs protect lung epithelial cells from the cytotoxic effects of α-toxin.

To determine how IFNα protects cells from α-toxin, we evaluated the early events following exposure to α-toxin. IFNα pretreatment did not decrease oligomerization of α-toxin, activation of p38 mitogen-activated protein (MAP) kinase, and efflux of potassium (Supplemental Figure S1). Within the first 30 min of α-toxin exposure, association of α-toxin with ADAM10 or recently reported α-toxin-induced ADAM10-dependent cleavage of E-cadherin (Inoshima et al., 2011) were not affected by IFNα pretreatment, albeit they were slightly reduced at 2 h (Supplemental Figure S1). To evaluate whether α-toxin triggers release of ATP into extracellular space, we treated A549 cells with α-toxin in the presence

of luciferin and luciferase in the medium. Following a short lag period, α-toxin triggered a robust increase in ATP-dependent luminescence peaking between 20 and 40 min with maximal luminescence intensity observed at 2.5 μg/ml of α-toxin (Figure 2A). Although many bacterial products such as endotoxin and staphylococcal peptidoglycan may trigger extracellular ATP (eATP) release (De Vuyst et al., 2007; Robertson et al., 2010), we found that α-toxin was a necessary and sufficient secreted factor of *S. aureus* for eATP release from lung epithelial cells: incubation of A549 cells with conditioned medium from α-toxin-producing *Hla⁺* strain of *S. aureus* triggered rapid and robust eATP release, which was virtually non-detectable after incubation with conditioned medium from isogenic *Hla⁻* α-toxin-mutant strain (Figure 2B). Thus, exposure of lung epithelial cells to α-toxin leads to eATP release.

We also measured eATP in the conditioned medium collected from cells at 15-min intervals after exposure to α-toxin, which allowed us to avoid luciferase inactivation by prolonged incubation at 37°C (Seminario-Vidal et al., 2009). The baseline eATP levels released by A549 cells within 1 h of culture under those conditions were below 20 nM and not affected by IFNα treatment. The concentrations of eATP peaked at 30 min after α-toxin and reached 1805±248 nM eATP. IFNα pretreatment did not change the kinetics of eATP release after α-toxin treatment, but significantly reduced peak eATP concentrations to 1341±170 nM (*p<0.01*, the data are mean±SEM of 7 independent experiments each performed in quadruplicate cultures). Treatment of human primary SAEC with α-toxin also triggered eATP release, albeit peak eATP concentrations were much lower than in A549 cells (Figure 2C). Importantly, IFNα pretreatment of SAEC significantly decreased eATP levels after α-toxin exposure.

The reduction in α-toxin-induced eATP concentrations in IFNα-pretreated cells could not be explained by changes in eATP hydrolysis. After 30-min incubation with 10-100 nM of exogenous ATP, the remaining ATP levels were similar between medium- and IFNα-pretreated cells. IFNα pretreatment actually slowed degradation of exogenously added ATP at 1000 nM concentration range (Figure 2D).

Extracellular nucleotides may contribute to cell lysis by bacterial pore-forming toxins through autocrine or paracrine activation of P2 receptors (Skals et al., 2009). We found that pretreatment of A549 cells with 500-1000 μM of oxidized ATP (a non-selective antagonist of P2 receptors) significantly inhibited α-toxin-induced cell death (Figure 2E). Moreover, oxidized ATP protected mice from hypothermia induced by intranasal administration of sublethal doses of α-toxin (Figure 2F). These data suggest that α-toxin-induced release of eATP and, probably other nucleotides, contribute to the cytotoxic effects of α-toxin via P2 receptors.

Identification of *PLSCR1* as a candidate gene involved in IFNα-induced protection from α-toxin

To characterize signaling pathways involved in IFNα-induced protection from α-toxin, we carried out a screening assay in A549 cells treated with IFNα, chemical inhibitors and α-toxin as depicted in Supplemental Figure S2. By measuring remaining intracellular ATP after α-toxin treatment as the readout, we found that IFNα-induced protection from α-toxin was not affected by inhibitors of caspase-1 (Ac-YVAD-FMK, 10 μM), sterol response element binding proteins (25-OH-cholesterol, 50 μM), ERK MAP-kinase (UO126, 10 μM) and EGFR tyrosine kinase (AG1478, 15 μM) (Figure S2). Inhibitors of caspases (zVAD-FMK as a pan-caspase inhibitor, 10 μM), gene transcription (actinomycin D, 2.5 μg/ml), protein synthesis (cycloheximide, 50 μg/ml) and removal of serum (i.e., treatment of cells in serum-free medium) showed moderate, but statistically significant protection of both medium- and IFNα-pretreated cells from α-toxin. However, inhibitors of p38-MAP kinase

(SB203580, 10 μM), PI3-kinase (LY294002, 10 μM), and fatty acid synthase (cerulenin, 10 μg/ml) significantly affected the protective effect of IFNα (Figure S2). Furthermore, inhibition of protein palmitoylation with 2-bromopalmitate (100 μM) effectively wiped out IFNα-induced protection from α-toxin (Figure 3A). The effects of 2-bromopalmitate were also evident when it was added to the cells 30 min after IFNα, i.e. approximately 24 h prior to α-toxin (Figure 3B). This treatment also sensitized A549 cells to α-toxin-induced cell death (Figure 3C), providing additional evidence for involvement of protein palmitoylation in protection of lung epithelial cells from α-toxin.

Using palmitoylation and regulation by type I IFNs as selection criteria, we analyzed the overlap between the 227 human genes associated with protein palmitoylation (Yang et al., 2010) and 218 IFN-regulated genes expressed in A549 cells (Sanda et al., 2006) and identified *FAS* (TNF receptor superfamily, member 6) and *PLSCR1* (Figure 3D). We dismissed *FAS* since interferons increase its expression, which is more likely to sensitize cells to FasL-mediated cell death than protect them from α-toxin (Chawla-Sarkar et al., 2003). Therefore, we focused our further analyses on *PLSCR1* since it is induced by type I IFNs (Zhou et al., 2000), palmitoylation of PLSCR1 protein directs it to lipid rafts in plasma membrane (Wiedmer et al., 2003), where α-toxin preferentially binds (Valeva et al., 2006; Wilke and Bubeck Wardenburg, 2010), and PLSCR1 is abundantly expressed by macrophages and neutrophils (Chen et al., 2011; Zhou et al., 2002), which are highly resistant to α-toxin-induced cell death (Valeva et al., 1997).

To determine whether PLSCR1 is induced in lung epithelial cells, we analyzed PLSCR1 expression in medium- and IFNα-pretreated human primary SAEC and A549 cells. At the baseline, PLSCR1 was hardly detectable; however, IFNα treatment led to robust induction of PLSCR1 protein (Figure 3E). PLSCR1 localized primarily in a perinuclear region, albeit some nuclear and membrane staining was also evident. Remarkably, following incubation of IFNα-pretreated cells with α-toxin for 2 h, most of the endocytosed α-toxin co-localized with a fraction of PLSCR1 (Figure 3F). Thus, IFNα-induced PLSCR1 may be in proximity with α-toxin.

PLSCR1 is necessary for IFNα-induced protection from α-toxin

To examine the role of PLSCR1 in IFNα-induced protection from α-toxin, we suppressed its induction by transfecting cells with PLSCR1-specific shRNA. A non-silencing (NS) control shRNA had no effect on PLSCR1 expression, whereas PLSCR1-specific shRNA further decreased the baseline and prevented IFNα-induced expression of PLSCR1 (Figures 4A and 4B). Furthermore, PLSCR1-specific shRNA did not affect baseline and IFNα-induced expression of STAT1 (Figures 4A and 4C). NS shRNA had no effect on α-toxin-induced ATP depletion in medium- or IFNα-pretreated A549 cells to α-toxin (Figure 4D). However, PLSCR1-specific shRNA negated the protective effects of IFNα on α-toxin-induced depletion of ATP (Figure 4D). Furthermore, PLSCR1-specific shRNA attenuated IFNα-induced protection from α-toxin-induced cell death (Figures 4E and Supplemental Figure S3). These data suggest that induction of PLSCR1 is necessary for IFNα-induced protection from α-toxin.

To explore the role of PLSCR1 in responses to α-toxin *in vivo*, we treated PLSCR1-knockout (PLSCR1-/-) mice and littermate heterozygous (PLSCR1+/-) mice (Zhou et al., 2002) with α-toxin via intranasal route. PLSCR1 deficiency (Figure 4F) had no effect on the early α-toxin-induced hypothermia, but resulted in impaired recovery of body temperature (Figure 4G), suggesting that lack of PLSCR1 increases sensitivity of mice to inhaled α-toxin. Subsequently, we tested whether PLSCR1 deficiency alters the outcome of experimental staphylococcal pneumonia due to infection with α-toxin producing *Hla*[+] strain of *S. aureus* or isogenic α-toxin-mutant *Hla*[-] strain of *S. aureus*. When infected with 2.5×10^8

CFU of *Hla⁺ S. aureus*, a larger fraction of PLSCR1-/- mice developed moribund condition sooner than PLSCR1+/- littermates (Figure 4H). Infection with *Hla⁺* resulted in severe hypothermia at 6 h post infection (p.i.) in PLSCR1+/- and PLSCR1-/- mice (Figure 4I). Among the survivors at 16 h p.i., 3 PLSCR1-/-mice and 7 PLSCR+/- mice started recovering their body temperature. These mice eventually survived the infection with *Hla⁺ S. aureus*. Transient and less severe hypothermia was observed in PLSCR1+/- and PLSCR1-/- mice infected with the *Hla⁻* strain (3.65×10^8 CFU/mouse). Importantly, all mice recovered their body temperature by 16 h and none of the mice were moribund within 72 h p.i. with *Hla⁻ S. aureus.* These data indicate that PLSCR1 deficiency increases sensitivity of mice to live α-toxin-producing *S. aureus*.

Effects of IFNα and α-toxin on scrambling of membrane phospholipids, eATP release, and PLSCR1 subcellular localization

Since PLSCR1 has been implicated in non-specific bidirectional translocation (scrambling) of membrane phospholipids (Stout et al., 1997), we evaluated whether IFNα pretreatment alters translocation of membrane phospholipids after α-toxin exposure. Binding of annexin V, which indicated exposure of phosphatidylserine on cell surface, significantly increased after treatment with α-toxin in medium-, but not in IFNα-pretreated cells (Figure 5A). In addition, we used FM1-43, a fluorescent reporter for plasma membrane phospholipid scrambling (Zweifach, 2000). Exposure of medium and IFNα-pretreated cells to α-toxin showed significantly increased binding of FM1-43; albeit the increase was less dramatic in IFNα-pretreated cells (Figure 5B). Thus, two independent assays showed that increased expression of PLSCR1 in IFNα-pretreated cells does not correlate with translocation of membrane phospholipids after α-toxin exposure.

To define how PLSCR1 mediates IFNα-induced protection from α-toxin, we measured eATP release from A549 cells stably expressing NS or PLSCR1-specific shRNA. In the absence of IFNα pretreatment, A549 cells stably expressing NS or PLSCR1-specific shRNA released similarly high levels of eATP in response to α-toxin (Figures 5C and 5D). Pretreatment with IFNα significantly reduced eATP release from the cells expressing NS shRNA. However, the response to IFNα pretreatment was attenuated in the cells expressing PLSCR1-specific shRNA. These data indicated that IFNα-induced PLSCR1 is necessary for reduction of eATP release after exposure to α-toxin.

Nuclear translocation of PLSCR1 augments transcriptional responses to type IFNs and G-CSF (Chen et al., 2011; Dong et al., 2004). To provide further insight into how IFNα-induced PLSCR1 may protect cells from α-toxin, we analyzed subcellular protein fractions for the presence of PLSCR1 after treatment with IFNα and/or α-toxin. Following IFNα pretreatment, PLSCR1 accumulated in the nuclear, membrane, and cytoskeleton-associated fractions (Figure 5E). Treatment with α-toxin had no effect on the amounts of PLSCR1 in the nuclear fractions (Figure 5E, top panel). Following exposure to α-toxin, membrane-associated PLSCR1 decreased in medium-pretreated cells, but increased in IFNα-pretreated cells (Figure 5E, medium panel). Remarkably, treatment with α-toxin led to sustained increases of PLSCR1 in the cytoskeleton-associated fractions, both in the medium- and IFNα-pretreated cells (Figure 5E, bottom panel). Moreover, immunofluorescence analyses of PLSCR1 after IFNα-pretreatment and exposure to α-toxin showed co-localization of PLSCR1 and F-actin (detected by phalloidin staining) in a subset of cells (Figure 5F and Supplemental Figure S4). In summary, these results indicated that exposure to α-toxin does not lead to nuclear translocation of PLSCR1, but results in accumulation of PLSCR1 in the cytoskeleton-associated protein fractions, at least in some cells.

Using wild-type PLSCR1 and PLSCR1 with mutations in palmitoylation sites or in nuclear localization signal (Wiedmer et al., 2003; Chen et al., 2005), we analyzed whether

overexpression of PLSCR1 may be sufficient to protect cells from α-toxin. Overexpressed wild-type PLSCR1 localized primarily to the nucleus, albeit some diffuse extranuclear expression of PLSCR1 was also observed (Supplemental Figure S4). Similar subcellular localization was observed for PLSCR1 with the mutations in the palmitoylation sites (184AAAPAA189, further referred as C-A mutant, Figure S4). The mutations in the nuclear localization signals (K258A, K261A/H263A, further referred as K-A mutant) excluded PLSCR1 from the nucleus (Figure S4). To evaluate the effects of these expression constructs on responses to α-toxin, we sorted transiently transfected cells by flow cytometry using the GFP marker in the bicistronic pMIG-IRES-GFP vector. Although we easily obtained more than 98% GFP$^+$ populations of cells with >94% post-sort cell viability for cells expressing wild-type and K-A-mutant PLSCR1, we were not able to obtain sufficient numbers of viable A549 cells transfected with the C-A mutant PLSCR1. We also could not produce stably transfected A549 cells expressing this construct, which suggested that expression of palmitoylation-deficient PLSCR1 in A549 cells may result in toxicity. When we treated the sorted A549 cells with α-toxin, we found that wild-type or K-A mutant PLSCR1 decreased release of eATP at 30 min after α-toxin (Figure 5G). Moreover, A549 cells overexpressing PLSCR1 or K-A PLSCR1 retained more ATP at 16 h after α-toxin treatment (Figure 5H). Thus, regardless of PLSCR1 nuclear localization, its overexpression is sufficient to replicate the effects of IFNα on cell responses to α-toxin.

Discussion

Our results show that exposure of human lung epithelial cells to α-toxin leads to eATP release into extracellular space. Importantly, IFNα protects human lung epithelial cells from α-toxin by reducing eATP release and allowing cells to maintain sufficient levels of intracellular ATP. To identify pathways and IFN-regulated genes involved in protection from α-toxin, we used a screening assay and bioinformatics analyses. As a result, we found that protein palmitoylation and induction of PLSCR1 are necessary to reduce ATP depletion and cell death.

Using PLSCR1-specific RNA interference, we demonstrated that induction of PLSCR1 is necessary for INFα-induced protection from α-toxin. Our experiment with PLSCR1-/- mice also suggested that PLSCR1 is involved in host responses to α-toxin *in vivo*. Importantly, PLSCR1 deficiency increased susceptibility of mice to the pulmonary infection with α-toxin-producing *S. aureus*. Thus, our findings reveal a function for PLSCR1 in protection of host cells from a bacterial pore-forming toxin.

Palmitoylation of PLSCR1 is required for localization of PLSCR1 to lipid rafts in the plasma membrane (Wiedmer et al., 2003), where it may contribute to nonselective translocation of phospholipids across the plasma membrane bilayer (Stout et al., 1997); albeit the latter notion is disputable (Bevers and Williamson, 2010). Non-palmitoylated PLSCR1 amplifies transcriptional responses to IFNα and G-CSF in the nucleus (Chen et al., 2011; Dong et al., 2004). As we observed increased levels of PLSCR1 in several subcellular compartments after IFNα pretreatment, it is possible that PLSCR1 contributes to induction of other IFN-regulated genes mediating protection from α-toxin. Due to potential toxicity of palmitoylation mutant PLSCR1 in A549 cells, we cannot completely rule out the possibility that non-palmitoylated PLSCR1 contributes to IFNα-induced protection from α-toxin. However, overexpression of K-A mutant PLSCR1, which is essentially excluded from the nucleus, was sufficient to replicate some of the IFNα effects, such as eATP release and retaining intracellular ATP. Thus, extranuclear PLSCR1 has cytoprotective functions.

In addition, we observed that exposure of cells to α-toxin led to colocalization of PLSCR1 with endocytosed α-toxin and polymerized F-actin, and accumulation of PLSCR1 in the

cytoskeleton-associated protein fractions. Binding of α-toxin to ADAM10 on lung epithelial cells impairs actin cytoskeleton (Wilke and Bubeck Wardenburg, 2010), whereas disruption of actin cytoskeleton by cytochalasin D prevents repair of α-toxin pores in fibroblasts and sensitizes them to α-toxin (Valeva et al., 2000). Furthermore, endocytosis, "detoxification" and exocytosis of α-toxin are important mechanisms of cellular resistance to α-toxin (Husmann et al., 2009). We did not observe co-immunoprecipitation of PLSCR1 with α-toxin, ADAM10 or F-actin (not shown). Thus, PLSCR1 is likely to protect cells from α-toxin without disruption of α-toxin-interaction with ADAM10. Our findings place PLSCR1 in a highly relevant subcellular compartments and call for further characterization of PLSCR1 functions and potential interacting molecular partners in this context.

We also showed that α-toxin triggers rapid, robust and sustained release of eATP, which was partially inhibited by IFNα-pretreatment in a PLSCR1-dependent manner. Extracellular nucleotides regulate lung barrier functions, survival activation and recruitment of epithelial cells and leukocytes (Eckle et al., 2009; Junger, 2011); and we found that oxidized ATP, a non-selective antagonist of P2 receptors, protected cells and mice against α-toxin. Therefore, further studies targeting release of extracellular nucleotides and/or purinergic receptor signaling should help determine the roles of extracellular nucleotides in pathogenesis of staphylococcal infections.

In conclusion, our study describes an innate immune program downstream of type I IFNs that induces PLSCR1 and mediates protection of host cells from death caused by a bacterial pore-forming toxin. This potentially beneficial process is apparently distinct from previously described deleterious effects of type I IFNs during bacterial infections (Carrero et al., 2004; Martin et al., 2009). Additional studies will be necessary to investigate the role of PLSCR1 during *in vivo* infections with live *S. aureus*.

Experimental Procedures

Reagents

We purchased staphylococcal α-toxin (specific activity 30,000 hemolytic units per mg) from List Biological Laboratories, human recombinant IFNα (specific activity at least 2×10^8 U/mg) from PBL InterferonSource, calcein-AM, and ethidium homodimer (EthD-1) from Invitrogen, SB203580, UO126, AG1478, LY294002, actinomycin D, and cycloheximide from EMD Biochemicals, cerulenin and 2-bromo-palmitate from Sigma.

Cell Cultures

We purchased A549 cells from ATCC and SAEC (derived from three separate donors) from ATCC and Lonza and cultured them according to manufacturers' recommendations. For functional assays, we seeded SAEC or A549 cells at 10,000 cells/well in 96-well plates, pretreated the cells with human recombinant IFNα (1000 U/ml) for 24 h, changed the culture medium and added diluted α-toxin or conditioned medium from *S. aureus* cultures. To obtain conditioned medium from *S. aureus* cultures, we inoculated single colonies into 10 ml of tryptic soy broth (TSB), cultured the bacteria for 24 h, pelleted them by centrifugation at 3000 *g* for 10 min and sterilized the supernatants with 0.22-μM filters (Millipore). *Hla⁺* strain of *S. aureus* (DU5617) and its isogenic *Hla⁻* mutant DU5618 were a generous gift from Dr. Timothy Foster (Trinity College, Dublin) (O'Reilly et al., 1986).

Assessment of cell death

To measure α-toxin-induced cell death in cultured cells, we stained live cells with 1 μM calcein AM and dead cells with 8 μM EthD-1 (Invitrogen). We omitted calcein AM staining in experiments with shRNA since fluorescence of GFP expressed from the vector clearly

marked live cells. We acquired images from random fields in at least 4 individual wells per group using inverted fluorescent microscope DMIRB (Leica) with 20X/0.40 objective, DC350FX camera (Leica) ImagePro software and manually counted live (green) and dead (red) cells. In some experiments, we measured death of A549 cells harvested by trypsinization using exclusion of trypan blue and TC10 automated cell counter (Bio-Rad) or using exclusion of 7-amino-actinomycin D (BD Biosciences) and flow cytometry.

Assessment of intracellular ATP

To measure cellular ATP after α-toxin treatment, we added equal volume of CellTiter Glo® reagent (Promega) to the wells with cells in the medium and, following 10-min incubation at room temperature with shaking, transferred the lysates to opaque LumiTrac plates (Greiner) and measured luminescence intensity using a Synergy HT plate reader (BioTek). We adjusted the sensitivity of the detector every time to remain in the linear mode. We normalized luminescence intensity from IFNα or α-toxin treated cells to the luminescence intensity from cells treated with medium alone.

Screening assay and bioinfomatics analyses

Following pretreatment of A549 cells with IFNα for 24 h, we pretreated cells with a panel of 20 commercially inhibitors of signaling pathways for 30 min and treated cells with α-toxin (0.5 and 2.5 μg/ml). We used carrier solutions (DMSO or ethanol) or negative control chemicals (i.e., zFA-FMK for zVAD-FMK) for control groups. After exposure to α-toxin for 16 h, we measured relative intracellular ATP as described above. To determine the interaction between the inhibitors and IFNα-pretreatment, we compared the remaining relative ATP levels after α-toxin treatment with or without the inhibitor (normalized to cells incubated in complete medium with carrier solution but without α-toxin) using two-way ANOVA assay.

To identify candidate genes involved in IFN-induced protection from α-toxin, we compiled the list of palmitoylation-associated human genes using published studies (Yang et al., 2010) and gene ontology records in Genbank http://www.ncbi.nlm.nih.gov/genbank/). We found the overlap between this list and the list of IFN-regulated genes expressed in A549 cells (Sanda et al., 2006) using Biovenn web application (Hulsen et al., 2008).

Measurement of eATP release

For detection of eATP release in real time, we diluted luciferin/luciferase reagent from the ATP Bioluminescence Assay Kit CLS II (Roche) in phenol red free and serum free DMEM medium (Invitrogen) and added it directly to SAEC and A549 cell cultures for 5 min. Following this equilibration period, we added α-toxin or diluted conditioned medium from *S. aureus* cultures and measured luminescence intensity every min for up to 60 min at 37°C.

To measure eATP concentrations, we cultured cells with α-toxin in phenol red free and serum free DMEM medium for the indicated time points and collected conditioned medium with a multichannel pipet into U-bottom microtiter plates kept on ice. Following a 5-min centrifugation at 300 g at 4°C, we transferred cell-free supernatants (25 μl) into plates prefilled with 25 μl/well CellTiter Glo® reagent (Promega) and measured luminescence intensity using a Synergy HT plate reader following 10-min incubation at room temperature with shaking. To generate the standard curves, we diluted ATP standards (Teknova) fresh every time in the culture medium.

Assessment of translocation of membrane phospholipids

We treated A549 cells plated in clear bottom 96-well plates with IFNα and α-toxin as indicated above. At the indicated time points, we stained the cells with diluted annexin V

labeled with Cy5.5 (BD Biosciences), washed the cells and scanned the plates with Odyssey imaging system (LICOR) using its 700-nm channel. Alternatively, we added lipophilic dye FM1-43 (5 μg/ml) to the cells after treatment with IFNα and α-toxin and measured its uptake after 5 min incubation with the Synergy plate reader using 508/20-nm excitation filter and 640/40-nm emission filter.

Knockdown and overexpression of PLSCR1 in A549 cells

PLSCR1-specific shRNA and control non-silencing shRNA subcloned into pLMP-IRES-GFP vector were a generous gift from Drs. Peter Sims and Therese Wiedmer (University of Rochester Medical Center). The PLSCR1-specific shRNA targets positions 1231-1252 within PLSCR1 mRNA (Genbank accession number NM_021105.2). The stem of the hairpin in the NS shRNA shows no homology to known human mRNA's. We stably transfected A549 cells with the shRNA-expressing vectors with Lipofectamine and maintained established clones (4 for each shRNA construct) in the presence of puromycin. Palmitoylation C-A mutant and nuclear localization KA mutant (Wiedmer et al., 2003; Chen et al., 2005) were subcloned into pMIG-IRES-GFP vectors and obtained from Drs Sims and Wiedmer. We overexpressed these mutant PLSCR1 and wild-type PLSCR1 by transiently transfecting A549 cells with FuGENE HD (Roche Applied Science) and sorting GFP+ cells using Sony-iCyt Reflection sorter at the Cell Sorter Core Facility (Yale University School of Medicine).

Subcellular fractionation and immunoblotting

For total protein lysates, we scraped cells from 100-mm dishes in lysis buffer containing 1 % Igepal (Sigma) and cleared cell lysates by centrifugation at 14,000 g for 10 min at 4°C. We isolated subcellular protein fractions using Subcellular fractionation kit from Pierce. For immunoblotting, we separated proteins in 4-15% precast gradient gels (Biorad), transferred onto nitrocellulose membranes, blocked and incubated with primary and near infrared fluorescently labeled secondary antibodies using reagents and protocols from LICOR. We scanned and analyzed immunoblots using Odyssey imaging system (LICOR).

Immunofluorescence

We seeded cells into 8-well LabTek chamber slides and treated them with IFNα and/or α-toxin for the indicated times. We washed cells with warm PBS containing calcium and magnesium, fixed with 4% paraformaldehyde, blocked with 10% FBS or normal goat serum, permeabilized with 0.1% Triton X-100 and stained with the indicated antibodies for PLSCR1 or α-toxin. We used Alexa Fluor-488-conjugated phalloidin to visualize polymerized F-Actin and DAPI for nuclear counterstaining. We acquired images using DMIRB microscope with 20X/0.75 objective, DC350FX camera (Leica) and ImagePro software or Nikon Eclipse 80i epifluorescence microscope with Retiga 2000R camera and NIS Elements software.

In vivo experiments

All studies with animals were carried out following a protocol approved by Yale University IACUC. We purchased C57BL/6 mice from the animal production facility of National Cancer Institute and PLSCR1+/- mice (F1 hybrids of C57BL/6 and 129 strains) from Texas Institute of Genomic Medicine (Zhou et al., 2002). We crossed PLSCR1+/-mice to obtain F2 littermate wild-type, heterozygous and homozygous PLSCR1-knockout mice. Since wild-type and heterozygous mice showed no apparent difference in PLSCR1 expression levels (not shown), we used sex-matched heterozygous mice as controls for knockouts. To evaluate the responses of mice to inhaled α-toxin, we anesthetized mice with isoflurane and administered 50 μl of sterile PBS containing sublethal doses of α-toxin (50 μg/kg body

weight) via intranasal route. Where indicated we mixed oxidized ATP (0.335 μMole/mouse) or equivalent volume of PBS with α-toxin immediately prior to administration to mice. We measured body temperature prior to α-toxin and at the indicated time points with an infrared thermometer (Exergen). We euthanized all mice with CO_2 at the end of the experiments.

For infection with live *S. aureus*, we diluted overnight cultures of *S. aureus* 1:100 in 50 ml TSB, subcultured for 2 h, washed twice with sterile PBS, and resuspended the pellets in 1.5 ml of sterile PBS. We administered 50 μl of the bacterial suspension to isoflurane-anesthetized mice via intranasal route and determined the actual dose of live *S. aureus* by plating serial dilutions on TSB agar plates. We monitored mice at regular intervals for up to 72 h for the following signs of moribund condition: sustained hypothermia (body temperature <28°C for more than 1 h as measured by the infra-red thermometer), lethargy, dehydration, change in the color of mucous membranes, labored breathing. We determined that mice showing more than 3 of the indicated signs were moribund and euthanized them promptly with CO_2. The time of developing this moribund condition was recorded to plot the survival curves.

Statistical analyses

In experiments involving more than two experimental groups, we determined whether the difference between the groups was statistically significant using one-way analysis of variance test and Bonferroni post test. Otherwise, we used two-tailed student's t-test. We analyzed the differences in body temperature between the groups of infected mice using Kruskal-Wallis nonparametric test followed by Dunn's post test for all groups. We analyzed the survival curves using the log-rank (Mantel-Cox) test. To perform all calculations we used GraphPad Prism software, version 4 (GraphPad Software, San Diego, CA).

Supplementary Material

Refer to Web version on PubMed Central for supplementary material.

Acknowledgments

References

Bartlett AH, Foster TJ, Hayashida A, Park PW. Alpha-toxin facilitates the generation of CXC chemokine gradients and stimulates neutrophil homing in Staphylococcus aureus pneumonia. J. Infect. Dis. 2008; 198:1529–1535. [PubMed: 18823272]

Bevers EM, Williamson PL. Phospholipid scramblase: an update. FEBS Lett. 2010; 584:2724–2730. [PubMed: 20302864]

Bhakdi S, Tranum-Jensen J. Alpha-toxin of Staphylococcus aureus. Microbiol. Rev. 1991; 55:733–751. [PubMed: 1779933]

Bubeck Wardenburg J, Schneewind O. Vaccine protection against Staphylococcus aureus pneumonia. J. Exp. Med. 2008; 205:287–294. [PubMed: 18268041]

Carrero JA, Calderon B, Unanue ER. Type I interferon sensitizes lymphocytes to apoptosis and reduces resistance to Listeria infection. J. Exp. Med. 2004; 200:535–540. [PubMed: 15302900]

Chawla-Sarkar M, Lindner DJ, Liu YF, Williams BR, Sen GC, Silverman RH, Borden EC. Apoptosis and interferons: role of interferon-stimulated genes as mediators of apoptosis. Apoptosis. 2003; 8:237–249. [PubMed: 12766484]

Chen MH, Ben-Efraim I, Mitrousis G, Walker-Kopp N, Sims PJ, Cingolani G. Phospholipid scramblase 1 contains a nonclassical nuclear localization signal with unique binding site in importin alpha. J. Biol. Chem. 2005; 280:10599–10606. [PubMed: 15611084]

Chen CW, Sowden M, Zhao Q, Wiedmer T, Sims PJ. Nuclear phospholipid scramblase 1 prolongs the mitotic expansion of granulocyte precursors during G-CSF-induced granulopoiesis. J. Leukoc. Biol. 2011; 90:221–233. [PubMed: 21447647]

Craven RR, Gao X, Allen IC, Gris D, Bubeck Wardenburg J, McElvania-Tekippe E, Ting JP, Duncan JA. Staphylococcus aureus alpha-hemolysin activates the NLRP3-inflammasome in human and mouse monocytic cells. PLoS One. 2009; 4:e7446. [PubMed: 19826485]

De Vuyst E, Decrock E, De Bock M, Yamasaki H, Naus CC, Evans WH, Leybaert L. Connexin hemichannels and gap junction channels are differentially influenced by lipopolysaccharide and basic fibroblast growth factor. Mol. Biol. Cell. 2007; 18:34–46. [PubMed: 17079735]

Dong B, Zhou Q, Zhao J, Zhou A, Harty RN, Bose S, Banerjee A, Slee R, Guenther J, Williams BR, et al. Phospholipid scramblase 1 potentiates the antiviral activity of interferon. J. Virol. 2004; 78:8983–8993. [PubMed: 15308695]

Eckle T, Koeppen M, Eltzschig HK. Role of extracellular adenosine in acute lung injury. Physiology (Bethesda). 2009; 24:298–306. [PubMed: 19815856]

Gurcel L, Abrami L, Girardin S, Tschopp J, van der Goot FG. Caspase-1 activation of lipid metabolic pathways in response to bacterial pore-forming toxins promotes cell survival. Cell. 2006; 126:1135–1145. [PubMed: 16990137]

Hulsen T, de Vlieg J, Alkema W. BioVenn - a web application for the comparison and visualization of biological lists using area-proportional Venn diagrams. BMC Genomics. 2008; 9:488. [PubMed: 18925949]

Husmann M, Beckmann E, Boller K, Kloft N, Tenzer S, Bobkiewicz W, Neukirch C, Bayley H, Bhakdi S. Elimination of a bacterial pore-forming toxin by sequential endocytosis and exocytosis. FEBS Lett. 2009; 583:337–344. [PubMed: 19101547]

Husmann M, Dersch K, Bobkiewicz W, Beckmann E, Veerachato G, Bhakdi S. Differential role of p38 mitogen activated protein kinase for cellular recovery from attack by pore-forming S. aureus alpha-toxin or streptolysin O. Biochem. Biophys. Res. Commun. 2006; 344:1128–1134. [PubMed: 16643845]

Idone V, Tam C, Andrews NW. Two-way traffic on the road to plasma membrane repair. Trends Cell Biol. 2008; 18:552–559. [PubMed: 18848451]

Inoshima I, Inoshima N, Wilke GA, Powers ME, Frank KM, Wang Y, Bubeck Wardenburg J. A Staphylococcus aureus pore-forming toxin subverts the activity of ADAM10 to cause lethal infection in mice. Nat. Med. 2011; 17:1310–1314. [PubMed: 21926978]

Junger WG. Immune cell regulation by autocrine purinergic signalling. Nat. Rev. Immunol. 2011; 11:201–212. [PubMed: 21331080]

Kallen AJ, Mu Y, Bulens S, Reingold A, Petit S, Gershman K, Ray SM, Harrison LH, Lynfield R, Dumyati G, et al. Health care-associated invasive MRSA infections, 2005-2008. JAMA. 2010; 304:641–648. [PubMed: 20699455]

Kennedy AD, Bubeck Wardenburg J, Gardner DJ, Long D, Whitney AR, Braughton KR, Schneewind O, DeLeo FR. Targeting of alpha-hemolysin by active or passive immunization decreases severity of USA300 skin infection in a mouse model. J. Infect. Dis. 2010; 202:1050–1058. [PubMed: 20726702]

Martin FJ, Gomez MI, Wetzel DM, Memmi G, O'Seaghdha M, Soong G, Schindler C, Prince A. Staphylococcus aureus activates type I IFN signaling in mice and humans through the Xr repeated sequences of protein A. J. Clin. Invest. 2009; 119:1931–1939. [PubMed: 19603548]

McCormick CC, Caballero AR, Balzli CL, Tang A, O'Callaghan RJ. Chemical inhibition of alpha-toxin, a key corneal virulence factor of Staphylococcus aureus. Invest. Ophthalmol. Vis. Sci. 2009; 50:2848–2854. [PubMed: 19136695]

Menzies BE, Kernodle DS. Passive immunization with antiserum to a nontoxic alpha-toxin mutant from Staphylococcus aureus is protective in a murine model. Infect. Immun. 1996; 64:1839–1841. [PubMed: 8613399]

O'Reilly M, de Azavedo JC, Kennedy S, Foster TJ. Inactivation of the alpha-haemolysin gene of Staphylococcus aureus 8325-4 by site-directed mutagenesis and studies on the expression of its haemolysins. Microb. Pathog. 1986; 1:125–138. [PubMed: 3508485]

Prevost G, Mourey L, Colin DA, Menestrina G. Staphylococcal pore-forming toxins. Curr. Top. Microbiol. Immunol. 2001; 257:53–83. [PubMed: 11417122]

Ragle BE, Bubeck Wardenburg J. Anti-alpha-hemolysin monoclonal antibodies mediate protection against Staphylococcus aureus pneumonia. Infect. Immun. 2009; 77:2712–2718. [PubMed: 19380475]

Ratner AJ, Hippe KR, Aguilar JL, Bender MH, Nelson AL, Weiser JN. Epithelial cells are sensitive detectors of bacterial pore-forming toxins. J. Biol. Chem. 2006; 281:12994–12998. [PubMed: 16520379]

Robertson J, Lang S, Lambert PA, Martin PE. Peptidoglycan derived from Staphylococcus epidermidis induces Connexin43 hemichannel activity with consequences on the innate immune response in endothelial cells. Biochem. J. 2010; 432:133–143. [PubMed: 20815816]

Rose F, Dahlem G, Guthmann B, Grimminger F, Maus U, Hanze J, Duemmer N, Grandel U, Seeger W, Ghofrani HA. Mediator generation and signaling events in alveolar epithelial cells attacked by S. aureus alpha-toxin. Am. J. Physiol. Lung. Cell. Mol. Physiol. 2002; 282:L207–214. [PubMed: 11792625]

Sanda C, Weitzel P, Tsukahara T, Schaley J, Edenberg HJ, Stephens MA, McClintick JN, Blatt LM, Li L, Brodsky L, Taylor MW. Differential gene induction by type I and type II interferons and their combination. J. Interferon Cytokine Res. 2006; 26:462–472. [PubMed: 16800785]

Schreiber MP, Chan CM, Shorr AF. Bacteremia in Staphylococcus aureus pneumonia: Outcomes and epidemiology. J. Crit. Care. 2011; 26:395–401. [PubMed: 21036521]

Seminario-Vidal L, Lazarowski ER, Okada SF. Assessment of extracellular ATP concentrations. Meth. Mol. Biol. 2009; 574:25–36.

Skals M, Jorgensen NR, Leipziger J, Praetorius HA. Alpha-hemolysin from Escherichia coli uses endogenous amplification through P2X receptor activation to induce hemolysis. Proc. Natl. Acad. Sci. USA. 2009; 106:4030–4035. [PubMed: 19225107]

Stout JG, Basse F, Luhm RA, Weiss HJ, Wiedmer T, Sims PJ. Scott syndrome erythrocytes contain a membrane protein capable of mediating Ca2+-dependent transbilayer migration of membrane phospholipids. J. Clin. Invest. 1997; 99:2232–2238. [PubMed: 9151796]

Valeva A, Hellmann N, Walev I, Strand D, Plate M, Boukhallouk F, Brack A, Hanada K, Decker H, Bhakdi S. Evidence that clustered phosphocholine head groups serve as sites for binding and assembly of an oligomeric protein pore. J. Biol. Chem. 2006; 281:26014–26021. [PubMed: 16829693]

Valeva A, Walev I, Gerber A, Klein J, Palmer M, Bhakdi S. Staphylococcal alpha-toxin: repair of a calcium-impermeable pore in the target cell membrane. Mol. Microbiol. 2000; 36:467–476. [PubMed: 10792732]

Valeva A, Walev I, Pinkernell M, Walker B, Bayley H, Palmer M, Bhakdi S. Transmembrane beta-barrel of staphylococcal alpha-toxin forms in sensitive but not in resistant cells. Proc. Natl. Acad. Sci. U S A. 1997; 94:11607–11611. [PubMed: 9326657]

Wiedmer T, Zhao J, Nanjundan M, Sims PJ. Palmitoylation of phospholipid scramblase 1 controls its distribution between nucleus and plasma membrane. Biochemistry. 2003; 42:1227–1233. [PubMed: 12564925]

Wilke GA, Bubeck Wardenburg J. Role of a disintegrin and metalloprotease 10 in Staphylococcus aureus alpha-hemolysin-mediated cellular injury. Proc. Natl. Acad. Sci. U S A. 2010; 107:13473–13478. [PubMed: 20624979]

Yang W, Di Vizio D, Kirchner M, Steen H, Freeman MR. Proteome scale characterization of human S-acylated proteins in lipid raft-enriched and non-raft membranes. Mol. Cell. Proteomics. 2010; 9:54–70. [PubMed: 19801377]

Yarovinsky T, Monick M, Husmann M, Hunninghake G. Interferons increase cell resistance to staphylococcal {alpha}-toxin. Infect. Immun. 2008; 76:571–517. [PubMed: 18070901]

Zhou Q, Zhao J, Al-Zoghaibi F, Zhou A, Wiedmer T, Silverman RH, Sims PJ. Transcriptional control of the human plasma membrane phospholipid scramblase 1 gene is mediated by interferon-alpha. Blood. 2000; 95:2593–2599. [PubMed: 10753839]

Zhou Q, Zhao J, Wiedmer T, Sims PJ. Normal hemostasis but defective hematopoietic response to growth factors in mice deficient in phospholipid scramblase 1. Blood. 2002; 99:4030–4038. [PubMed: 12010804]

Zweifach A. FM1-43 reports plasma membrane phospholipid scrambling in T-lymphocytes. Biochem. J. 2000; 349:255–260. [PubMed: 10861236]

Highlights

◆ IFNα decreases cell death triggered by staphylococcal α-toxin

◆ IFNα reduces α-toxin-induced release of ATP into extracellular space

◆ Phospholipid scramblase 1 is required for IFN-induced protection from α-toxin

◆ Phospholipid scramblase 1 accumulates in the cytoskeleton fraction
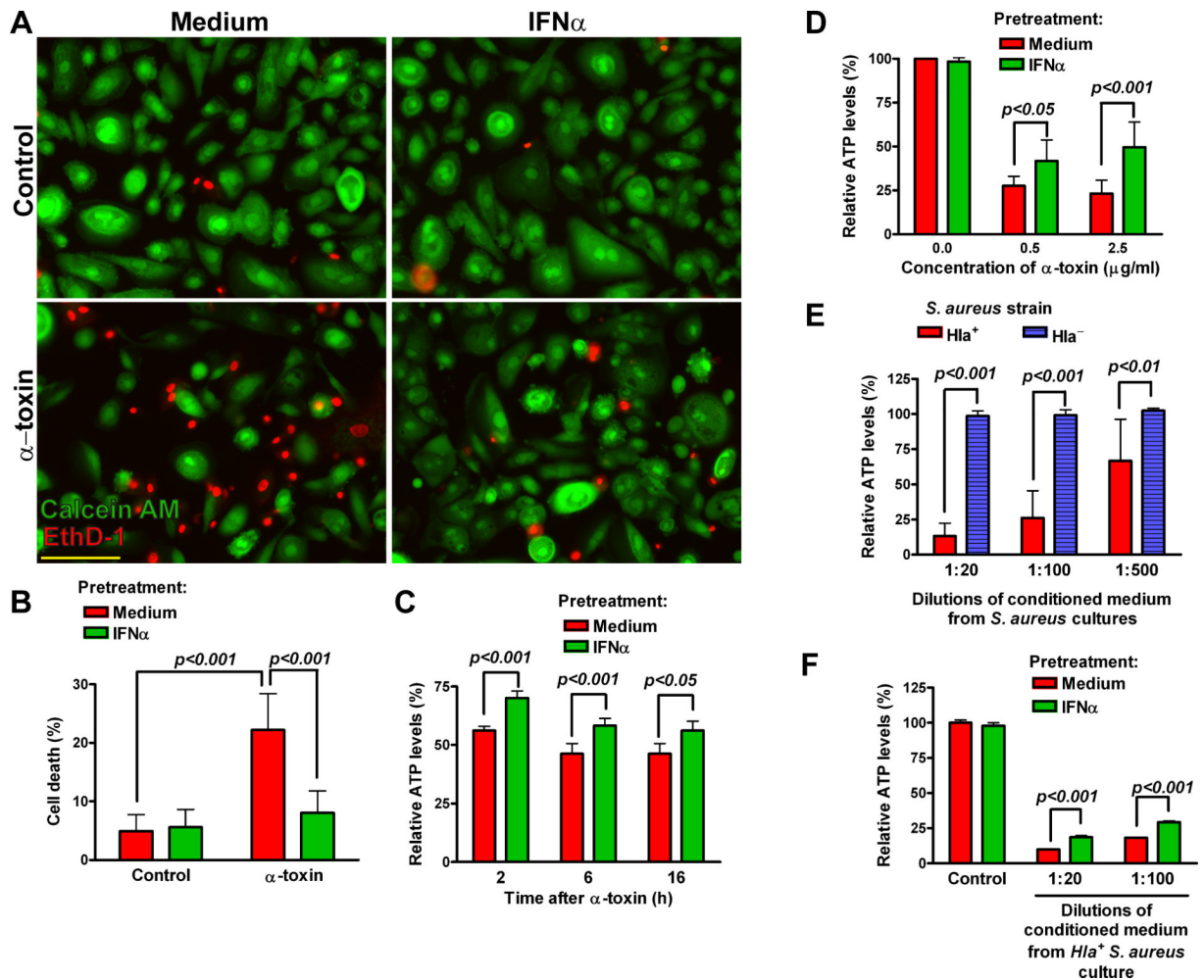
Figure 1.

IFNα protects lung epithelial cells from α-toxin-induced cell death and depletion of intracellular ATP. Human primary SAEC were pretreated with medium or IFNα (1000 U/ml) for 24 h and treated with α-toxin (0.1 µg/ml) for additional 24 h. (A): Representative photomicrographs of cells stained with calcein AM (green, live) and EthD-1 (red, dead); scale bar = 100 µM. (B): Percent dead cells (mean±SD of five independent experiments, each carried out in quadruplicate wells). (C): Relative levels of intracellular ATP (% remaining, relative to untreated cells at each time point) were measured in SAEC at the indicated time points after α-toxin (mean±SD of quadruplicate wells, the data are representative of five experiments). (D): Relative ATP levels in IFNα-pretreated A549 cells at 6 h after α-toxin (mean±SD of five independent experiments, each carried out in quadruplicate wells). (E) and (F): Relative ATP levels in medium- or IFNα-pretreated A549 cells after incubation with conditioned medium (diluted 1:100) from cultures of *Hla⁺* or *Hla⁻ S. aureus*. The data (mean±SD of quadruplicate wells) are representative of three independent experiments.
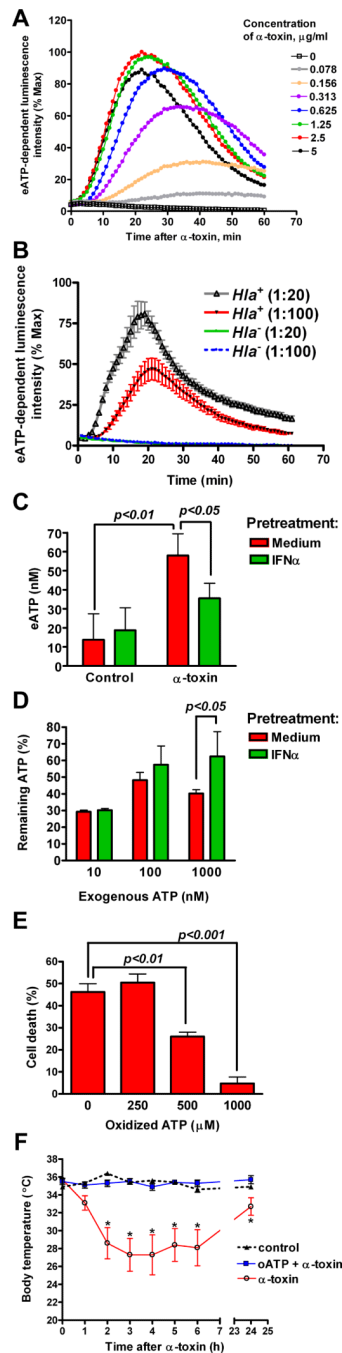
Figure 2.

Exposure to α-toxin triggers release of eATP that is inhibited by IFNα-pretreatment. A549 cells were treated with the indicated concentrations of α-toxin (A) or diluted conditioned medium from cultures of *Hla⁺* or *Hla⁻ S. aureus* (B). The curves show normalized mean luminescence intensity kinetics measured every minute within 1 h after α-toxin. Data in (A) are mean of quadruplicate cultures and are representative of two independent experiments. Data in (B) are mean±SEM of triplicate cultures and are representative of three independent experiments. (C): SAEC were pretreated with IFNα for 24 h and exposed to 0.1 μg/ml α-toxin for 30 min. Cell-free conditioned medium was used to measure eATP. The data are mean±SD of quadruplicate cultures and are representative of three independent experiments.

(D): Exogenous ATP was added to medium- or IFNα-pretreated A549 cells for 30 min. Cell-free conditioned medium was used to measure remaining ATP (% input, the data are mean±SD of quadruplicate cultures and are representative of three experiments). (E): A549 cells were pretreated with oxidized ATP for 2 h prior to exposure to 2.5 μg/ml α-toxin. Cell death at 24 h after α-toxin is shown. The data are mean±SD of quadruplicate cultures and are representative of three independent experiments. (F): C57BL6/ mice (8-wk old, females) were administered α-toxin or α-toxin with oxidized ATP diluted in 50 μl sterile PBS via intranasal route. Body temperature was measured at the indicated time points. The data are mean±SD, n=5. Control mice received 50 μl sterile PBS. Asterisks indicate the time points when the body temperature in mice treated with α-toxin alone was significantly lower than in other groups of mice ($p<0.05$).
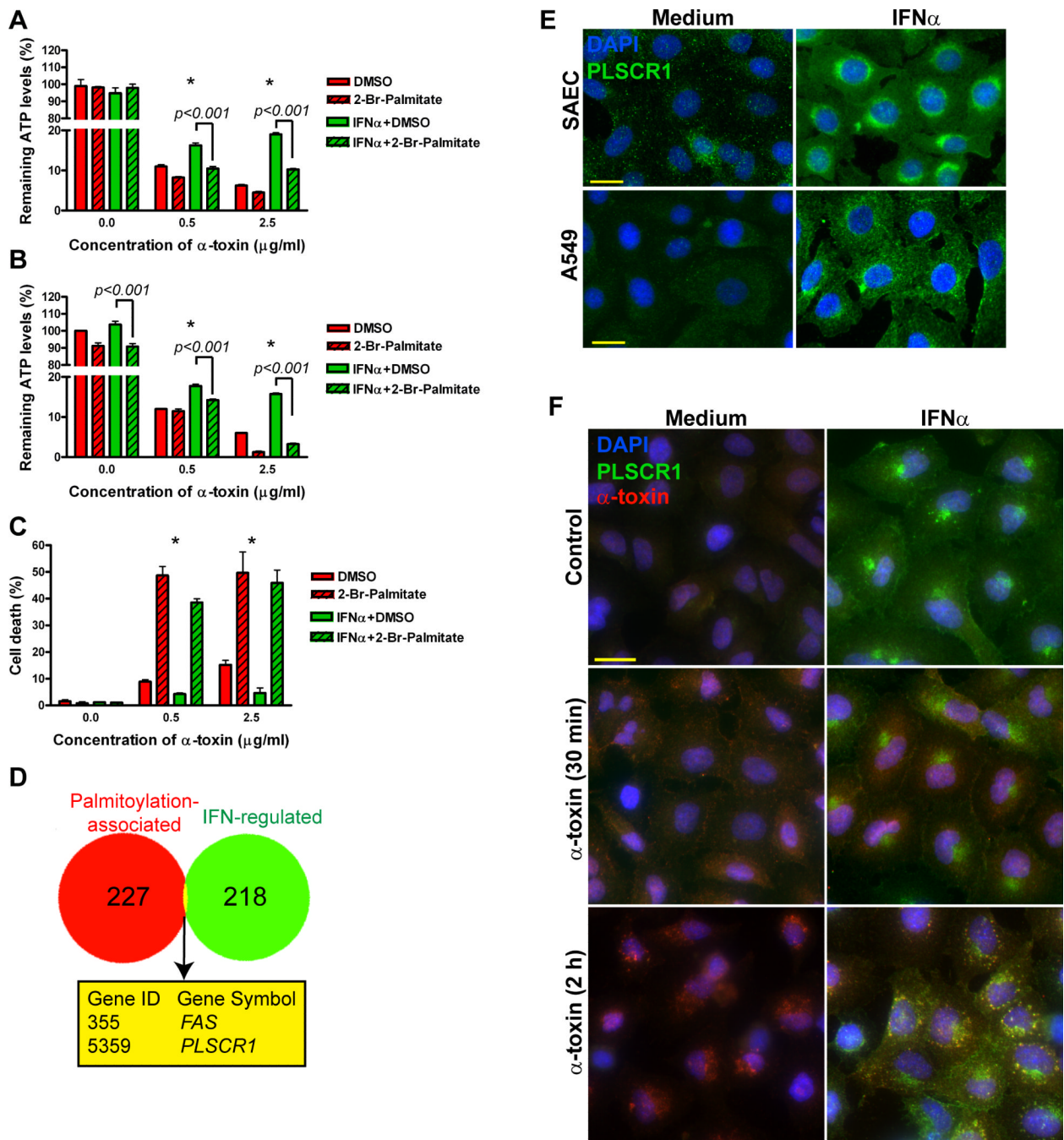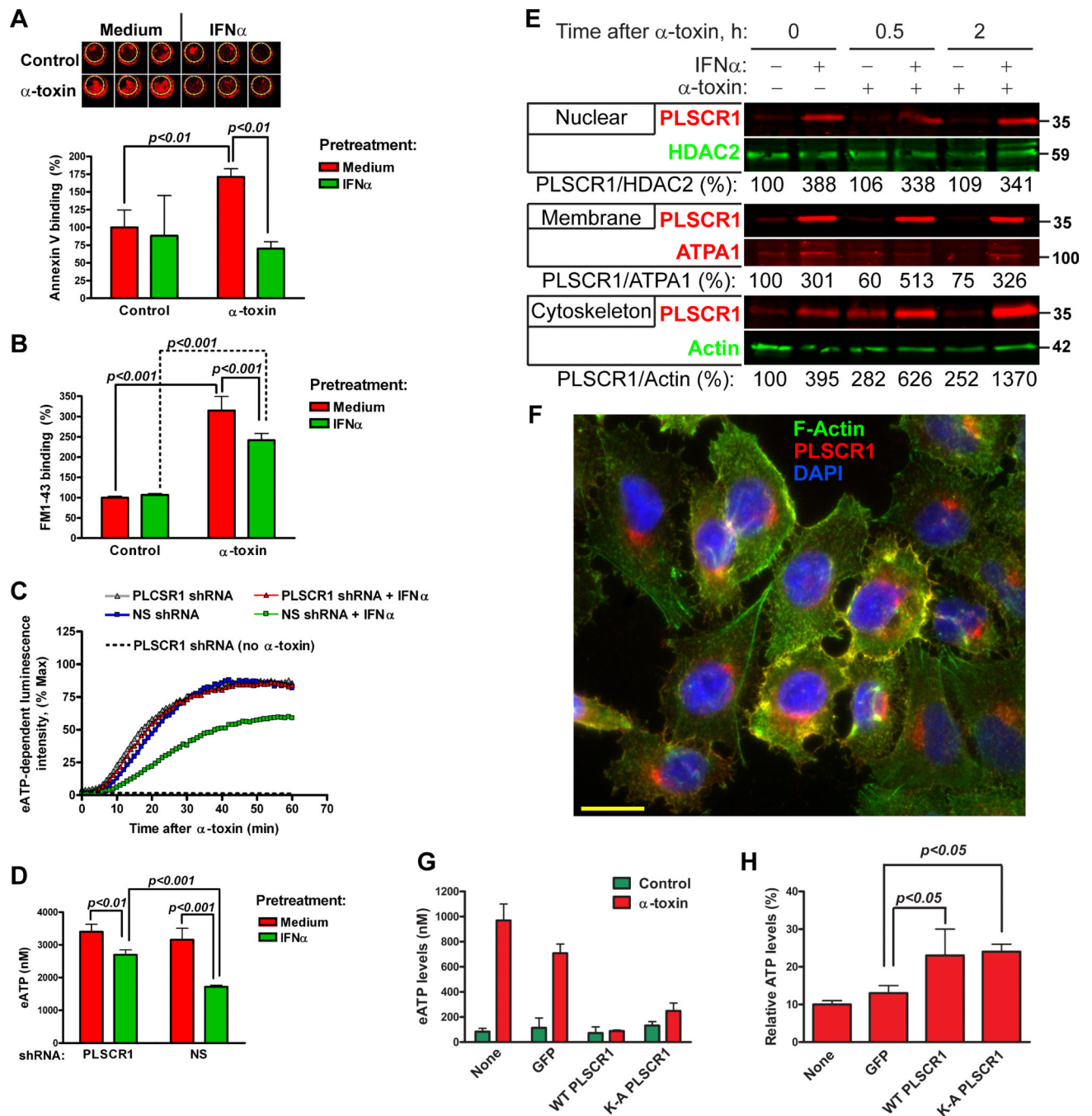
Figure 3.
Identification of PLSCR1 as a candidate gene involved in IFNα-induced protection from α-toxin. Medium- or IFNα-pretreated A549 cells were incubated with 2-bromopalmitate 30 min prior to α-toxin (A) or 30 min after IFNα (i.e., approximately 24 h prior to α-toxin (B and C). Relative ATP levels remaining after 16-h treatment with α-toxin are shown in (A) and (B) (mean±SD of quadruplicate cultures normalized to ATP levels in A549 cells pretreated with medium and DMSO without α-toxin). (C): Cell death measured by staining with 7-amino-actinomycin D and flow cytometry after 24-h treatment with α-toxin. The data are mean±SD of triplicate cultures. Asterisks indicate statistically significant interaction between 2-bromopalmitate and IFNα pretreatment at the indicated concentration of α-toxin

(p<0.005). (D): Venn diagram showing the overlap between IFN-regulated genes expressed in A549 cells and genes associated with protein palmitoylation. (E): SAEC and A549 cells were treated with 1000 U/ml IFNα for 24 h and analyzed for expression of PLSCR1 by immunofluorescence. (F): Medium and IFNα-pretreated A549 cells were exposed to 2.5 μg/ml of α-toxin at 37°C for 30 min or 2 h, washed twice, fixed, permeabilized and stained with mouse anti-human PLSCR1 and rabbit anti-α-toxin antibodies followed by secondary antibodies (goat anti-mouse conjugated with Alexa Fluor-488 and goat anti-rabbit conjugated with Alexa Fluor-647). Representative photomicrographs from three independent experiments are shown; scale bar = 20 μM.
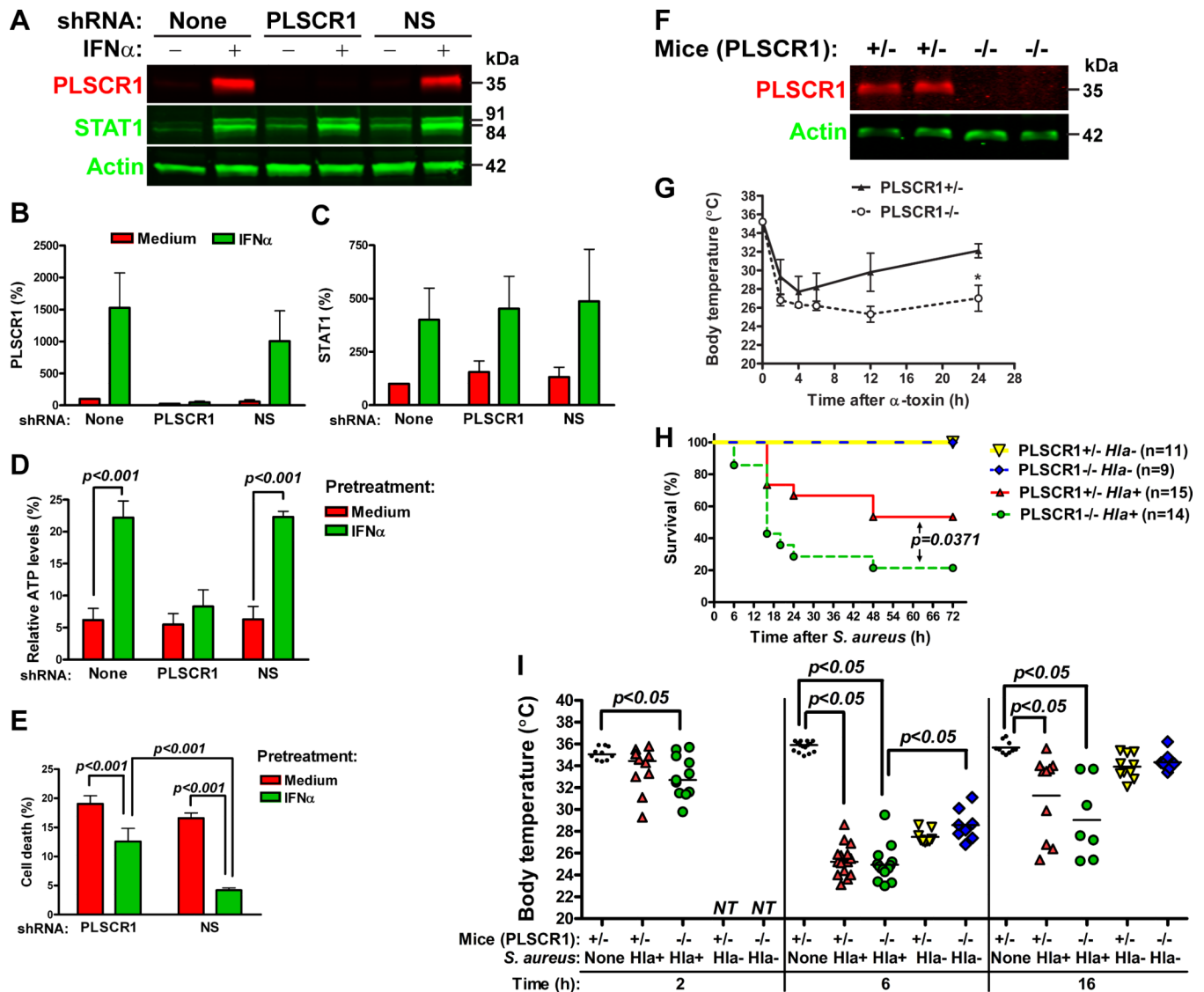
Figure 4.
Expression of PLSCR1 is necessary for INFα-induced protection from α-toxin. A549 cells were stably transfected with PLSCR1-specific or non-silencing (NS) shRNA vectors and analyzed for expression of PLSCR1 and STAT1 by immunoblotting. A representative immunoblot (A) and densitometry analyses of PLSCR1 (B) and STAT1 (C) expression normalized to actin are shown (mean±SD of three independent experiments). A549 cells stably expressing PLSCR1-specific or NS shRNA were pretreated with IFNα and treated with 2.5 μg/ml α-toxin. (D): Relative ATP levels remaining after 16-h treatment with α-toxin. The data are mean±SD of three independent experiments. (E): Cell death after 24-h treatment with α-toxin. The data are mean±SD of quadruplicate cultures and are representative of three experiments. (F): Immunoblot analysis of PLSCR1 expression in the lungs of littermate PLSCR1+/- and PLSCR1-/- mice. (G): Littermate PLSCR1-/- and PLSCR1+/- mice were administered α-toxin via intranasal route. Body temperature was measured at the indicated time points. Asterisk indicates statistically significant difference in body temperature between the groups at 24 h after α-toxin (mean±SEM, *p<0.05*, n=4). (H): Littermate PLSCR1-/- and PLSCR1+/- mice were infected with 2.5×10⁸ CFU/mouse of α-toxin-producing *Hla⁺ S. aureus* or 3.65×10⁸ CFU/mouse of isogenic α-toxin-deficient *Hla⁻*

S. aureus and monitored for the signs of moribund condition for up to 72 h. (I): Body temperature for control non-infected mice and *S. aureus*-infected mice at 2, 6 and 16 h post infection is shown (median and individual values, NT - not tested).

Figure 5.
Effects of IFNα and α-toxin on scrambling of membrane phospholipids, eATP release and
PLSCR1 subcellular localization. Translocation of membrane phospholipids was analyzed in
A549 cells pretreated with medium or IFNα for 24 h and treated with 2.5 μg/ml α-toxin.
(A): Binding of Cy5.5-labeled annexin V to phosphatidylserine on cell surface was
measured by LICOR Odyssey imaging system. Representative images and normalized
integrated fluorescence intensity at 2 h after α-toxin are shown. The data are mean±SD of
triplicate cultures and are representative of three independent experiments. (B): Uptake of
lipophilic fluorescent dye FM1-43 at 2 h after α-toxin. Normalized fluorescence intensity is
shown. The data are mean±SD of triplicate cultures and are representative of three

independent experiments. A549 cells stably expressing PLSCR1-specific or non-silencing (NS) shRNA were pretreated with IFNα and exposed to 2.5 μg/ml α-toxin. (C): Kinetics of eATP release. The curves represent normalized mean luminescence intensity of quadruplicate cultures. (D): Concentration of eATP in the culture medium at 30 min after α-toxin (mean±SD of quadruplicate cultures). The data are representative of three independent experiments. (E): Subcellular protein fractions were obtained from A549 cells pretreated with medium or IFNα and treated with α-toxin for the indicated time points and analyzed for expression of PLSCR1 by immunoblotting. Representative immunoblots and normalized densitometry values from two independent experiments are shown. (F): Immunofluorescence staining for PLSCR1 and phalloidin staining for F-Actin in A549 cells after IFNα pretreatment and α-toxin exposure for 30 min. A representative photomicrograph from two independent experiments is shown; scale bar = 20 μM. A549 cells were transfected with plasmids expressing GFP alone, wild-type PLSCR1 or nuclear localization mutant K-A PLSCR1, sorted for GFP coexpression, replated and treated with α-toxin. (G): Release of eATP was measured at 30 min after α-toxin. (H): Total cellular ATP was measured at 16 h after α-toxin and normalized to total cellular ATP without α-toxin treatment. The data are mean±SD of quadruplicate cultures and are representative of two independent experiments.